ACS OMEGA

Open Access

http://pubs.acs.org/journal/acsodf

Article

Development of Nanostructured Lipid Carrier-Loaded Flavonoid-Enriched *Zingiber officinale*

Sharifah Sarah Shazwani, Anita Marlina,* and Misni Misran*

Cite This: *ACS Omega* 2024, 9, 17379−17388

Read Online

ACCESS | Metrics & More | Article Recommendations | Supporting Information

ABSTRACT: Flavonoids, which are bioactive molecules found in *Zingiber officinale*, have been widely used as antioxidant and anti-inflammatory drugs. The presence of nanostructured lipid carriers (NLCs) as sophisticated delivery systems for bioactive compounds, such as flavonoids, can increase their bioavailability and stability, thus potentially producing better therapeutic effects. This study aimed to develop an anti-inflammatory topical gel using NLC-containing flavonoids derived from *Zingiber officinale*. The NLC formulation was prepared using stearic acid, a mixture of medium-chain triglycerides and isopropyl myristate, Tween 20, and Span 20 by using a hot homogenization method. The total flavonoid content obtained through sequential maceration stages was 4.04 mg of QUE/g of dry extract. The highest encapsulation efficiency of flavonoid-loaded NLC was observed at a flavonoid, *Zingiber officinale* extract (ZOE) concentration of 2%. It was found that a ZOE concentration of 0.4% provided excellent stability with a particle size of 302−344 nm and a polydispersity index of 0.14−0.23 after 28 days of observation. Morphological analysis of the ZOE-loaded NLC revealed a stable and well-developed formulation with a fairly uniform distribution. The presence of distinctive and uniformly distributed single particles suggests a promising alternative drug delivery system for conventional topical preparations. ZOE-loaded NLC gel showed solid-like properties and higher quality stability than the gel.

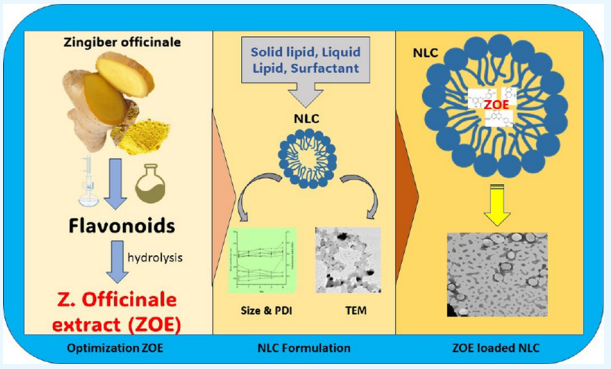

1. INTRODUCTION

Over the past few decades, there has been a notable surge in the consumption of synthetic antioxidants and anti-inflammatory agents, primarily due to their perceived advantages in large-scale manufacturing. However, concerns regarding the adverse effects and potential health risks associated with these synthetic bioactive compounds have prompted a shift toward exploring natural alternatives.[1] Numerous studies have been conducted on the extraction of active substances with anti-inflammatory[2−4] and antioxidant properties.[5−7] *Zingiber officinale*, also known as ginger, is a readily available plant that has been studied for this purpose. *Zingiber Officinale* var. rubrum is a plant belonging to the *Zingiberaceae* family and has been extensively employed as a traditional medicine globally, with a particular emphasis on its use in Asia.[8] This study focused on the distinctive approach of harnessing the bioactive potential of *Zingiber officinale* as a flavonoid and as a source of natural antioxidants and anti-inflammatory agents.

Flavonoids, including Kaempferol and Quercetin, exhibit potent anti-inflammatory activity by inhibiting inflammation mediators.[9−11] Flavonoids are classified into two primary types: glycosides and aglycones. In general, the absorption of topically administered flavonoid aglycones is superior to that of their equivalent glycosides because of their reduced molecular size and increased lipophilicity.[12] Despite the well-documented health benefits of flavonoids, their therapeutic effectiveness is hindered by challenges in their pharmacokinetic profile, such as their limited water solubility, poor bioavailability, and susceptibility to environmental factors.[13] Self-assembled colloidal lipid systems, particularly nanostructured lipid carriers (NLCs), have emerged as a promising solution. Previous studies have investigated the encapsulation of *Z. officinale* in NLCs using commercially available ginger oil,[14] red ginger extract,[15] and essential oils.[16]

NLCs, a second-generation form of lipid nanoparticles, possess a structure that enables the efficient transport of flavonoids into the body, thereby enhancing their absorption, therapeutic efficacy, permeability, bioavailability, solubility, reduced adverse effects, longer half-life, and tissue-targeted systemic delivery.[17−21] Comprising a binary mixture of solid and spatially liquid lipids, NLCs exhibit a disordered crystal matrix, providing ample space for accommodating active

Received: January 3, 2024
Revised: March 25, 2024
Accepted: March 28, 2024
Published: April 5, 2024

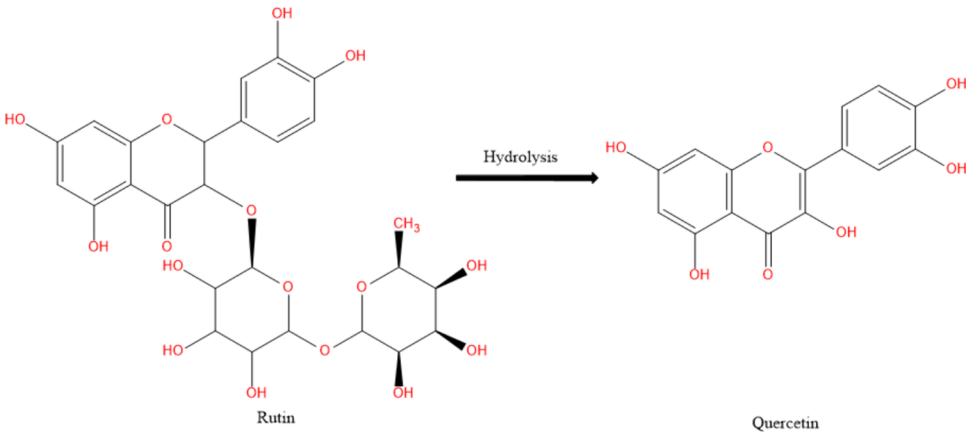

Figure 1. Bioconversion of rutin (glycosidic flavonoid) to quercetin (aglycone flavonoid) through deglycosilation. Reproduced with permission from ref 27. Available under a CC-BY 4.0 license. Copyright [2021] [Pharmaceutics].

molecules and leading to an enhanced drug loading capacity.[22,23] The liquid lipid content directly influences the ability of the lipids to remain in the solid state at body temperature, achieving controlled drug release. Moreover, NLCs can be further developed into several administration dosage forms, such as gels, creams, or ointments, which would aid in improving the phytochemical therapeutic line. Due to the impermeable nature of the skin, which makes it challenging to administer topical drugs,[24] NLC gel provides a great solution to optimize drug application via the topical route, ensuring close contact with the outermost layers of the skin and facilitating greater penetration of active molecules.[25]

To date, there have been no comprehensive studies on the incorporation of flavonoids obtained from the extraction of *Z. officinale* into NLC. Therefore, this study aimed to develop an anti-inflammatory topical gel using flavonoid-enhanced extract-loaded NLCs derived from *Z. officinale* to strategically address the limitations associated with conventional drug delivery systems such as poor solubility, inadequate bioavailability, and high toxicity. This research endeavors to substitute synthetic bioactive agents with natural constituents, such as flavonoids derived from *Z. officinale*, by assessing the effectiveness of three commonly used extraction techniques, namely, traditional maceration, Soxhlet extraction, and sequential maceration, to obtain the maximum yield of crude extracts from powdered *Z. officinale*. Furthermore, the process of obtaining flavonoid-enriched *Z. officinale* (ZOE) involved acid hydrolysis of the crude extract. Additionally, optimized NLCs loaded with flavonoid-enriched ZOE were integrated into a stable gel system to improve the efficacy of topical administration.

Anticipated benefits include improved stability, enhanced drug loading capacity, low systemic toxicity, prolonged half-life, and reduced adverse effects, making NLCs a promising platform for topical anti-inflammatory formulations. The comprehensive exploration of NLC technology seeks to optimize the anti-inflammatory potential of *Zingiber officinale* extracts, establish an efficient NLC drug carrier formulation, and create a natural-based anti-inflammatory topical formulation with an enhanced drug delivery system. This innovative approach emphasizes the unique contribution of this study to the broader context of drug delivery and bioactive compound utilization.

2. MATERIALS AND METHODS

2.1. Materials. Stearic acid, isopropyl myristate (IPM), Tween 20, Span 20, phosphate-buffered saline (PBS) tablets, and iota carrageenan were supplied by Sigma-Aldrich (St. Louis, MO, USA). Louis, MO, USA). Medium-chain triglycerides (MCT) were purchased from a local pharmacy (Caring Pharmacy, Malaysia). Anhydrous calcium chloride was purchased from Merck, and carboxymethyl cellulose (CMC) was obtained from Dai-Ichi Kogyo Seiyaku (Kyoto, Japan). *Zingiber officinale* rhizomes were purchased from Ethno Valley (Sg. Buloh, Malaysia). Deionized water with a resistivity of 18.2 cm^{-1} was used to prepare all solutions and samples and provided via a Barnstead Diamond Nanopure Water Purification unit connected to a Barnstead Diamond RO unit (Barnstead International, USA).

2.2. Methods. *2.2.1. Preparation of Flavonoid-Enriched Z. officinale Extract. 2.2.1.1. Extraction of Z. officinale.* *Zingiber officinale* extraction follows a systematic approach to obtain bioactive flavonoids. Two extraction techniques, Soxhlet extraction and traditional maceration, were employed using 70% ethanol as the solvent. Solute to solvent ratio of 1:5 was standardized for both techniques. The resulting ethanolic crude extracts were compared, and a more efficient method was selected for further investigation. This study addressed the critical issue of solvent selection by identifying a complex array of bioactive compounds in plants. The main goal of this method is to improve the extraction process by considering the different affinities of various compounds for solvents. Additionally, it yields the highest possible amount of crude extract and the most effective recovery of bioactive chemicals from plant sources. Two solvent systems were tested using the maceration technique: a monosolvent system using 70% ethanol and a sequential solvent extraction process involving hexane, dichloromethane, ethyl acetate, and 70% ethanol.[26] Each solvent was selected on the basis of its polarity, dielectric constant, and molecular structure. Following each extraction, the extracts were centrifuged at 10,000 rpm for 45 min, and the supernatant was separated. The remaining sediment was subjected to additional extraction using a solvent with a higher polarity. This sequential process involved the use of solvents with increasing polarities to optimize the flavonoid content of the crude extracts. The resulting fractions were evaporated under reduced pressure and stored at 4 °C until

https://doi.org/10.1021/acsomega.4c00091
ACS Omega 2024, 9, 17379−17388

further use. The yield percentage was calculated using the following formula:

$$\text{Yield\%} = \frac{\text{massofextract}}{\text{massofherb}} \times 100 \quad (1)$$

2.2.1.2. Acid Hydrolysis Reflux. To increase the biological activity of flavonoids, rutin was deglycosylated to quercetin using two different solvents and acid concentrations, as shown in Figure 1.[27] The crude extract was subjected to acid hydrolysis to maximize the yield of the flavonoid phytocompounds. The method used in this study involved the technique proposed by Yang et al.[28] Approximately 3 g of crude extract was weighed and dissolved in 80 mL of acidic solution of 80% ethanol and 0.5 M HCl in water. The solutions were heated to 75 °C for 3 h under continuous stirring. The excess solvent was removed via rotational evaporation.

2.2.1.3. Total Flavonoid Content Assay. The flavonoid content was determined using a Varian Cary 50-UV−visible spectrophotometer at a wavelength of 430 nm by using the colorimetric method. The colorimetric approach entails adding sodium nitrite, aluminum chloride, and sodium hydroxide to the sample.[29,30] First, a quantity of 1 mm of the material was solubilized in 5 mL of distilled water, as demonstrated by Azieana with slight modification.[31] The sample was introduced into a 0.3 mL solution of sodium nitrite ($NaNO_2$) at a concentration of 5% and incubated for 6 min. Subsequently, a volume of 0.3 mL containing 10% aluminum chloride ($AlCl_3$) was introduced into the sodium nitrite solution, followed by an incubation period of 5 min. The last step involved adding 2 mL of 1 M sodium hydroxide (NaOH). The mixture was vigorously agitated until it underwent a noticeable change in color, turning pink, which indicated the presence of flavonoids. Quercetin was employed as a reference compound in this investigation to establish a calibration curve ranging a concentration range of 10−1000 μg/mL. The total flavonoid content (TFC) was determined, and the results were expressed as quercetin equivalents (mg quercetin (QE)/g dried extract (DE)).

$$\text{TFC} = C \times \frac{V}{M} \quad (2)$$

where C is the concentration of quercetin (mg/mL), V is the volume of plant extract (mL), and M is the weight of crude plant extract (g). In this study, the total flavonoid content test was used to calculate the approximate difference in flavonoid (quercetin, mg/mL) concentrations in the extracts before and after acid hydrolysis.

2.2.1.4. High-Performance Liquid Chromatography Analysis. Flavonoid compounds were identified using high-performance liquid chromatography (HPLC; Shimadzu, Kyoto, Japan). The mobile phase consisted of 1% (v/v) aqueous acetic acid solution (solvent A) and acetonitrile (solvent B). The injection column was maintained at 20 L, and the flow rate was adjusted to 0.7 mL/min. The column was thermostatically controlled at 28 °C. The ratio of solvent B to solvent A was varied to achieve a gradient elution. The gradient elution was then altered in a linear fashion from 10 to 63% B for 11 min, with 63% sustained for 10 min. After 26 min, the elution was increased to 90%. The composition was restored to its original form (solvent B:solvent A, 10:90) after 31 min, and the system was operated for 5 min before injecting the next sample. The total analysis time per sample was 36 min.[32] HPLC chromatograms were obtained using a photodiode array UV detector calibrated at 272 nm. A Shimadzu Prominence LC-20AT high-performance liquid chromatography (HPLC) system (Kyoto, Japan) with an SPD-M20A UV−visible detector was used for the HPLC analysis. For reverse-phase separations of the flavonoid compounds, a Shim-pack C18 column (250 mm × 4.6 mm I.D., 5 m) was utilized (Thermo Scientific, Massachusetts, USA).

2.2.2. Anti-Inflammatory Assay (Nitric Oxide Assay). The nitric oxide (NO) inhibition assay was performed according to the procedure described by Boora et al.,[33] with minor modifications. To determine the nitrite radical scavenging activity of the extracts at different concentrations, 1 mL of the extract was mixed with approximately 0.5 mL of 10 mM Sodium Nitroprusside in phosphate buffer solution. The mixture was then incubated at room temperature for 15 min. Subsequently, equal amounts of the Griess reagent were added to the mixture. Quercetin was used as a positive control, and the absorbance at 378 nm was determined through UV−visible spectrophotometry. The nitrite radical scavenging activity of the extracts was calculated by using the following formula:

$$\text{Nitricoxideinhibition}(\%) = \frac{A_{\text{control}} - A_{\text{test}}}{A_{\text{control}}} \times 100 \quad (3)$$

where A_{control} represents the absorbance of the positive control and A_{test} represents the absorbance of the experimental samples.

2.2.3. Formulation of NLCs (Hot Homogenization Method). NLCs were prepared using high-shear and hot homogenization techniques. The NLC formulation was previously optimized through Box Behnken analysis, resulting in a highly efficient and effective product.[34] The composition comprises 2.9% stearic acid, 0.4% medium-chain triglycerides (MCT), 0.3% isopropyl myristate (IPM), 0.37% Tween 20, 0.23% Span 20, and 96% deionized water (DW). The lipid phase was heated in a water bath at 80 °C with constant stirring until the mixture became colorless. A preheated surfactant solution was mixed with the molten lipid phase and vigorously agitated at 18,000 rpm using a T25 basic homogenizer (IKA, Germany). NLCs are formed when hot emulsions are rapidly dispersed in cold water, which is typically maintained at approximately 2 °C. This process leads to the formation of a stable nanostructured lipid carrier system.[35]

2.2.4. Encapsulation of ZOE into Optimized NLCs. Different concentrations of *Z. officinale* (0.02, 0.04, 0.06, 0.08, and 0.1%) were introduced into the lipid phase mixture before heating and sonication to solubilize the active ingredient in the lipid mixture. A preheated aqueous surfactant solution was added to the molten lipid−drug mixture, followed by homogenization. The emulsion was carefully dispersed in cold water at approximately 4 °C to form NLC-encapsulated flavonoid-enriched ZOE.

The encapsulation efficiency (EE%) of the ZOE-loaded NLCs was determined by using an ultrafiltration technique with subsequent analysis using a UV−visible spectrophotometer (UV−vis Cary 50). Samples (5 mL) were introduced into a Vivaspin 6 tube and centrifuged at 8000 rpm for 1 h. This process aimed to separate free ZOE from ZOE-loaded NLCs. The supernatant containing unencapsulated *Z. officinale* was collected from the bottom chamber of the centrifuge tube and further analyzed by UV−vis spectrophotometry at 470 nm using two clear-sided quartz cuvettes with a 1 cm path length.

https://doi.org/10.1021/acsomega.4c00091
ACS Omega 2024, 9, 17379−17388

The EE% of each sample was determined using the following equation.

$$EE\% = \left(\frac{w_D - w_F}{w_D}\right) \times 100 \quad (4)$$

where W_D is the initial drug concentration in the NLCs, W_F is the concentration of unencapsulated or free drugs in the recovered supernatant, and W_L is the total lipid concentration of the NLCs.

2.2.5. Stability Observation of Optimized Loaded NLCs. Stability analysis was performed to evaluate the influence of storage on the average particle size, polydispersity index, and zeta potential of the formulation. These parameters were estimated in triplicate. The formulations were placed in an airtight container and stored at room temperature for 28 days. The particle size, polydispersity index (PDI), and zeta potential of each NLC formulation were measured using a Malvern Nano series Zetasizer (Malvern Instruments, UK) at 27 °C with a backscattering angle of 173°. Approximately 50 μL of NLCs was diluted in 5 mL of deionized water and filtered using a 0.45 μL PTFE membrane filter prior to measurement to ensure the absence of external debris and dust. The preparation of a highly dispersed and almost clear system is imperative for the mechanism of the dynamic light scattering technique used by the Malvern Nano series Zetasizer. A system with a high viscosity would cause a false interpretation of the multiple scattering of light by only one particle, because of the close distance between the particles. Each measurement was conducted three times to ensure the certainty of the results.

2.2.6. Transmission Electron Microscopy. The surface morphology of NLCs was visualized using TEM (Carl Zeiss Libra 120). Approximately three drops of the NLC solution were deposited onto a 400-mesh copper grid and left under ambient conditions for 3 min. The excess solution was removed by careful blotting on a filter paper. Two drops of 3% phosphotungstic acid stain were placed on the grid and left to air-dry at room temperature prior to TEM observation.

2.2.7. Development and Characterization of Gel. 2.2.7.1. Preparation of Gel Formulation. The gel was prepared by combining carboxymethyl cellulose with iotacarrageenan at a ratio of 7:3 with a 0.06% (w/w) calcium ion solution. To induce gelation and achieve the formation of a transparent gel, the mixture was thermally treated at approximately 80 °C.[36] Subsequently, the gel was incubated overnight to obtain the most favorable swelling level. A 30% (w/w) concentration of ZOE-loaded NLC was incorporated into the gel and homogenized for 1 min at 8000 rpm. The resulting mixture was stored at 4 °C until subsequent analysis.

2.2.7.2. Physicochemical Evaluation of Gels. The ZOE-loaded gel underwent several characterizations, including physical observations to detect signs of discoloration, phase separation, unusual smell, and changes in texture. In addition, the drug content and total yield were determined. The pH values were measured using an S47-K SevenMulti dual-meter pH/conductivity device (Mettler Toledo, Switzerland) after a storage period of 90 days.

$$Yield\% = \frac{praticalmass}{theoreticalmass} \times 100 \quad (5)$$

The gel, weighing approximately 1 g, was dissolved in 50 mL of methanol to determine the concentration of the active components. The solution was then centrifuged at 8000 rpm for 10 min. The resulting supernatant was filtered through a membrane filter with a pore size of 0.45 μm. Subsequently, the filtered solution was diluted in methanol and analyzed by using a UV−visible spectrophotometer (UV−vis Cary 50) to quantify its colorimetric characteristics.

$$Drugcontent\% = \frac{activeingredientconcentrationfromsupernatant}{initialaddedactiveingredientconcentration} \times 100 \quad (6)$$

2.2.8. Statistical Analysis. The findings are presented in the form of mean values accompanied by their corresponding standard deviations using Origin software. The data underwent statistical analysis, which was performed using one-way analysis of variance (ANOVA), with a significance level set at $p < 0.05$.

3. RESULTS AND DISCUSSION

3.1. Preparation of Flavonoid-Enriched *Zingiber officinale* Extract. *3.1.1. Extraction and Optimization of ZOE.* Two common extraction procedures, Soxhlet extraction and maceration, were employed to evaluate their efficacy in producing the maximum yield of the crude *Z. officinale* extract (mg/mL). As shown in Table 1, the Soxhlet extraction method

Table 1. Total Crude Extract Yield Was Determined Using the Soxhlet Method and Maceration

	extraction technique (total yield, g)		maceration with solvent system (total yield, g)	
samples	Soxhlet	maceration	ethanolic	sequential
rhizomes of *Z. officinale*	5.98	3.65	3.65	5.81

is a more efficient way to extract crude extracts than the traditional maceration method. This was supported by the fact that the amount of crude extract obtained through Soxhlet extraction was substantially higher than that obtained through traditional maceration. By applying a Soxhlet extraction, the solvent was repeatedly circulated through the sample using a reflux process. This allows for deeper penetration of the solvent into the plant material, resulting in the extraction of more compounds than maceration. Additionally, heating the solvent to its boiling point increases the solubility of the compound, resulting in better extraction than maceration at room temperature. However, excessive temperature application may result in a decrease in solutes, potentially causing unwanted impurity reactions and breakdown of thermolabile compounds.[37]

In order to extract bioactive chemicals known as flavonoids from *Zingiber officinale*, it is important to consider the extraction temperature, and the maceration technique was selected for the subsequent procedure. Furthermore, flavonoids are susceptible to heat and may undergo degradation and reduction in bioactivity when exposed to elevated temperatures.[38,39] The maceration procedure was carried out at room temperature by comparing two different solvents: a monosolvent (ethanol) and a sequential solvent. The latter involved four different solvents in ascending order of polarity: hexane, dichloromethane, ethyl acetate, and ethanol. Generally, the polarity index of the solvent used plays an active role in the extraction process, as the quantities of crude extracts differ depending on the solvent used.[40] By using solvents ranging

https://doi.org/10.1021/acsomega.4c00091
ACS Omega 2024, 9, 17379−17388

Table 2. Total Flavonoid Content, TFC, of *Z. officinale* Extracts Obtained Using Different Extraction Techniques

	TFC mg QUE/g dry extract		
samples	ethanolic extract	sequential extract (before acid hydrolysis)	sequential extract (after acid hydrolysis)
rhizomes of *Z. officinale*	2.46 ± 0.09	3.71 ± 0.06	4.04 ± 0.05

from nonpolar to polar, the amount of polar flavonoids present in the crude extract can be significantly increased. It was found that the use of a sequential solvent system resulted in a greater quantity of crude extracts containing flavonoids than the use of ethanol alone. This finding suggests that using sequential solvents with varying polarities, such as hexane, dichloromethane, ethyl acetate, and ethanol, is an effective and efficient method for extracting bioactive compounds, such as flavonoids, from plants.

As shown in Table 2, the total flavonoid content (TFC) of extracts obtained from ethanolic extraction is 2.46 ± 0.09 mg of QUE/g of DE, whereas the average total flavonoid content of extracts produced from sequential maceration is 3.71 ± 0.06 mg of QUE/g of DE. Optimization of the flavonoid content in ZOE by sequential maceration was carried out by employing acid hydrolysis reflux, which effectively facilitated the breakdown of superfluous chemicals and sugars. This deglycosylation process results in the conversion of glycosides to aglycones, which leads to the elimination of unnecessary low-molecular-weight sugars. Previous studies have reported that the highest quercetin content in peel extract increases by approximately 12 times after acid hydrolysis.[41] Following the acid hydrolysis reflux method, a significant rise in the TFC value was noted, with an increase of 4.04 mg ±0.05 QUE/g of DE.

3.1.2. High-Performance Liquid Chromatography Analysis. Figure 2 shows chromatograms of optimized ZOE before and after acid hydrolysis. A prominent peak was observed in the ZOE chromatogram after acid hydrolysis, appearing at a retention time of approximately 25 s. The observed peak was aligned with that associated with quercetin, a standard flavonoid molecule. Qualitatively, the content of quercetin in ZOE elevated 3-fold with an initial approximate amount of 1.34−4.1 mg/g DE after acid hydrolysis treatment. Therefore, quercetin in the optimized ZOE was effectively eluted at different retention periods during gradient and isocratic elution, using a mobile phase consisting of 1% (v/v) acetic acid and acetonitrile.

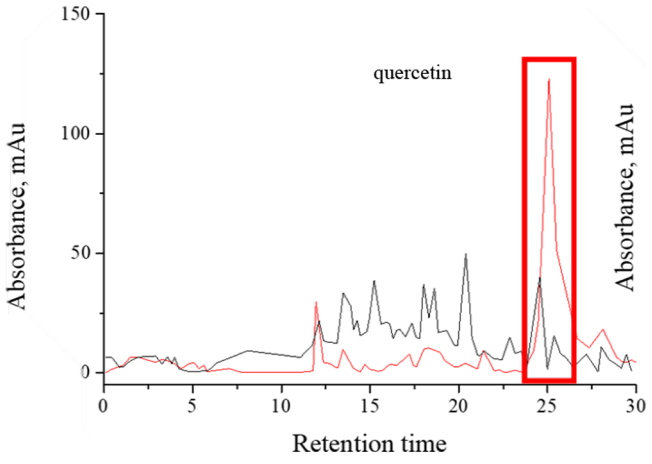

Figure 2. HPLC chromatogram of the optimized extract of *Z. officinale* before acid hydrolysis (top/black) and after having undergone acid hydrolysis (bottom/red).

3.1.3. Nitric Oxide Scavenging Assay. In this study, changes in the anti-inflammatory effects of glycoside acid hydrolysis reactions were investigated by using the Griess colorimetric test to measure the presence of nitrite and nitrate in the samples. Optimized ZOE showed moderately good nitric oxide scavenging activity against NO produced by sodium nitroprusside between 0.06 and 1 mg/mL (Table 3).

Table 3. Nitric Oxide (NO) Scavenging Percentage of the Quercetin-Standardized *Z. officinale* Extract

prepared concentration (mg/mL)	tested concentration (mg/mL)	average % inhibition	
		before acid hydrolysis	after acid hydrolysis
0.1 mg/mL (quercetin)		74.53 ± 0.39	
0.03125	0.015625	35.48 ± 1.24	41.91 ± 0.25
0.0625	0.03125	44.81 ± 1.06	46.19 ± 0.23
0.125	0.0625	46.22 ± 0.24	48.82 ± 1.39
0.25	0.125	46.92 ± 0.43	49.02 ± 0.22
0.5	0.25	48.09 ± 0.54	49.81 ± 0.72
1	0.5	48.83 ± 0.12	51.95 ± 0.51
2	1	52.65 ± 0.38	56.15 ± 0.64
Ic50		0.04 ± 0.00	0.04 ± 0.00

Overall, the percentage of inhibition increased with increasing extract concentrations. The standardized extract showed a nitric oxide scavenging activity of approximately 54% relative to the standard quercetin at similar concentrations (Table 3). With an IC50 efficacy of 0.042 mg/mL for ZOE, quercetin was 21 times more efficacious than the optimized extracts, which is acceptable considering that the tested samples were not isolated. Incubation of sodium nitroprusside solution in PBS at 25 °C resulted in linear time-dependent nitrite production, which was reduced by the tested extracts.[42]

3.2. Characterization of NLCs. *3.2.1. Encapsulation Efficiency, EE%.* The efficiency of encapsulation signifies the ability of NLCs to effectively include and safeguard bioactive compounds found in plant extracts. This process involves complex chemical interactions between the lipids that constitute the carriers and chemical constituents of the extracts. In this study, NLCs were incorporated with different concentrations of ZOE to determine the maximum quantity of flavonoid-rich ZOE that could be encapsulated. The encapsulation efficiency of flavonoid-rich ZOE in NLCs was directly proportional to the increased amount of the active ingredient until it reached the optimal loading amount, as shown in Figure 3. The encapsulation efficiency of the investigated loaded NLCs was highly satisfactory, with over 90% efficiency achieved at concentrations of 0.6−2%. The maximum encapsulation efficiency of flavonoid-rich ZOE in NLCs was achieved at a ZOE concentration of 2%, specifically yielding a value of 93.2%. Subsequently, as the concentration of ZOE was increased, the EE value decreased. This decrease can be attributed to the removal of ZOE from the NLCs or its redistribution among particles, resulting in a gradual reduction

https://doi.org/10.1021/acsomega.4c00091
ACS Omega 2024, 9, 17379−17388

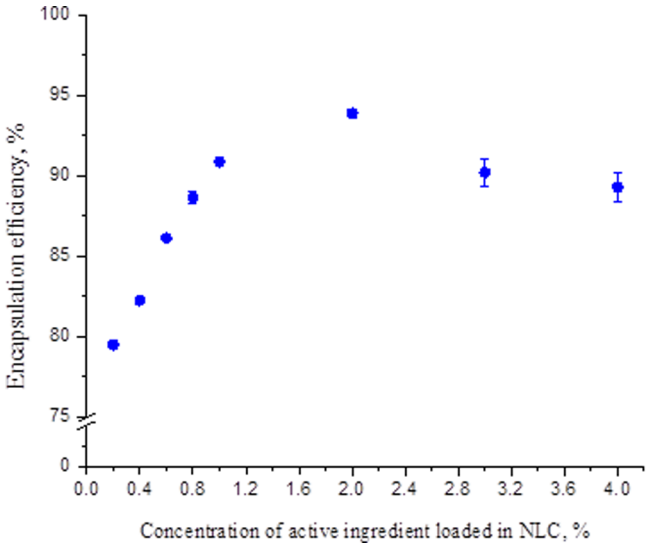

Figure 3. Encapsulation efficiency (%) of the NLC formulations containing various concentrations of active ingredients.

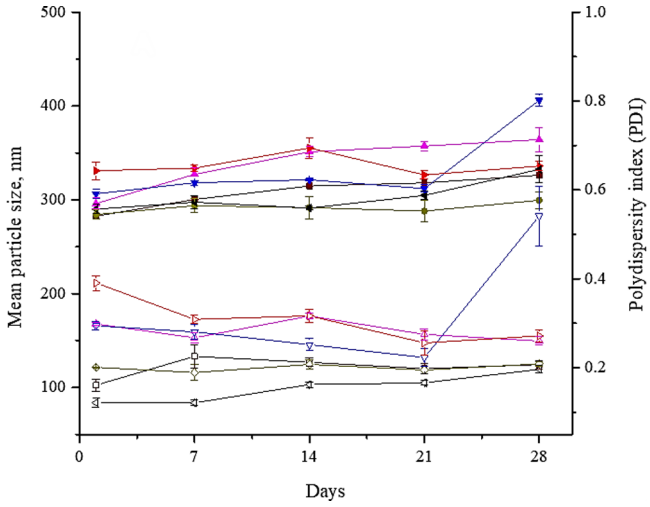

Figure 4. Particle size (solid symbol) and polydispersity index (PDI, open symbol) measurement of NLC formulation with 0% (◀), 0.2% (■), 0.4% (●), 0.6% (▲), 0.8% (▼), and 1% (▶) active ingredient content.

in the encapsulation efficiency. The efficiency of active ingredient encapsulation indicates a progressive increase until it reaches the ideal encapsulation percentage, after which it decreases.[43]

This outcome may be attributed to the hydrophobic nature of the major phytocompounds present in the optimized extracts, which play a crucial role by causing the extract to preferentially stay in the lipid matrix rather than the aqueous dispersing medium,[36] which disrupts the crystalline structure and increases the loading space. A high encapsulation efficiency ensures that a significant portion of these bioactive compounds is protected within the lipid matrix, shielding them from environmental factors and potential degradation.[44] Furthermore, this not only enhances the stability of the encapsulated compounds but also contributes to their controlled release, improving bioavailability and therapeutic efficacy.[45] The hydrophobic nature of the optimized extracts collectively contributed to the successful encapsulation and high efficiency of the NLC formulations.

3.2.2. Stability Studies of NLCs and ZOE-Loaded NLCs. The stability of the NLC system, including blank NLCs and ZOE-loaded NLCs, was assessed over a period of 28 days. This was achieved by evaluating the particle size and the polydispersity index. As shown in Figure 4, the blank NLCs had a particle size of 294.83 ± 0.4 nm on day 1 of storage and only exhibited small increments of 9.36% of the starting size during the 28 days, with no detectable sign of sample instability at ambient temperature and 4 °C, suggesting a stable formulation. A PDI measurement value consistently less than 0.2 further points to homogeneous particle dispersion. In response to imperfections, liquid lipids reduce the melting temperature of the lipid nanoparticles. Despite this, the amount of liquid lipid that can be added to NLCs is still constrained by temperature, highlighting the significance of NLCs maintaining their solid particles at least at a body temperature of 37 °C and ruling out the hypothesis that it is an oil-in-water dispersion.[46] According to Yew and Misran, the integration of liquid lipids greater than 30% of the lipid components was considered undesirable because an oil droplet detached from the NLC might be produced.[35]

The NLC formulation studied in this study was composed of a liquid lipid component, which accounted for 20% of the overall formulation. This liquid lipid component is composed of two primary ingredients, MCT and IPM, which are present in ratios of 42 and 58%, respectively. It is worth noting that the formulation remained consistently homogeneous and showed no physical changes, even after a prolonged storage period. The inclusion of MCT in the NLC formulation significantly reduced the surface tension of the solution. This lowered surface tension, in turn, leads to a decrease in the viscosity of the lipid phase, allowing for the formation of smaller particles.[47] This effect can be attributed to the ability of MCT to interact with lipid molecules and enhance their fluidity, resulting in better dispersion and emulsification of the formulation.

The amount of ZOE incorporated into the NLC is a crucial factor that affects the particle size, polydispersity index (PDI), and formulation stability, as depicted in Figure 4. In the initial stage, the particle size of NLCs containing flavonoid-enriched ZOE increased with increasing ZOE concentrations. Over 28 days, there were fluctuating changes in particle size; except for ZOE concentrations of 0.2 and 0.6%, there was a gradual increase in the particle size. NLCs with the highest ZOE content showed a consistent increase in mean particle size throughout the first half of the 28 day observation. Subsequently, there was a significant decrease, followed by a tendency to stabilize until the end of the observation period.

PDI measurements revealed fluctuations in the patterns of the formulations. This might be due to the occurrence of Ostwald ripening of the particles within the systems, which induces a sparse and poor distribution of particles, resulting in significant fluctuations in particle size and PDI measurements over the storage period.[48] These patterns may indicate changes in the composition or consistency of the formulation and could potentially have an impact on its effectiveness or stability. After 28 days of storage, there was a significant increase in the uniformity of the particle distribution at a ZOE concentration of 1%, as indicated by a decrease in the polydispersity index. The NLC formulations with ZOE concentrations of 0.8 and

https://doi.org/10.1021/acsomega.4c00091
ACS Omega 2024, 9, 17379−17388

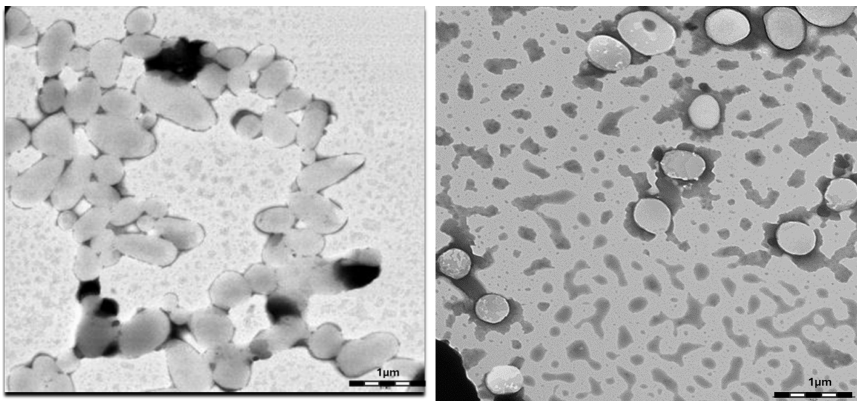

Figure 5. TEM micrograph of NLC formulation with no load (left) and loaded with 0.4% active ingredient (right) at 10,000× magnification.

Table 4. Physical Evaluation of Blank Gel, NLC Gel, and ZOE-NLC Gel Formulations at Room Temperature

					pH	
formulation	physical appearance	drug content (% w/w)	% yield	homogeneity	day 1	day 90
blank gel	transparent	NA	78.3	homogenous, no visible phase separation	6.31 ± 0.01	6.55 ± 0.06
NLC gel	cloudy	NA	76.1		5.22 ± 0.12	5.74 ± 0.08
ZOE-NLC gel	cloudy/semitransparent	74.0			5.53 ± 0.07	5.64 ± 0.02

1% exhibited the lowest PDI values on day 21, which corresponded to a reduction in particle size.

On day 14, the formation of specks of particles in the NLC formulations with 0.6, 0.8, and 1% ZOE was observed, which may explain the inconsistencies in the measurement of particle size and PDI. After the observation period, it was found that NLCs with a ZOE of 0.4% had the smallest and most consistent average particle size and PDI values. The particle sizes ranged from 302 to 344 nm, while the PDI values ranged from 0.143 to 0.234.

3.2.3. Morphology Observation of ZOE-Loaded NLCs. Visual observation of the optimized ZOE-loaded NLCs after 28 days of monitoring was performed by using transmission electron microscopy (TEM). As shown in Figure 5, the TEM micrograph of the blank NLCs exhibited an elongated shape and absence of separated oil droplets. This is because of the high liquid lipid content, which causes a disoriented matrix structure, thereby preventing a rigid, rounded shape.[35] High-pressure homogenization of NLCs might also result in the occurrence of shear stress, which consequently causes stretching of the particles and thus an elongated shape. However, upon the incorporation of the optimized extract into the matrix core of NLCs, the particles began to exhibit regular circular shapes and were relatively uniform, suggesting good particle dispersity. This suggests that ZOE significantly interacts with lipids, which helps stabilize the repulsion of hydrophobic groups in NLCs. The loaded NLCs exhibited no evidence of agglomeration, as the individual particles were consistently dispersed throughout the TEM images. It is important to ensure that there is no agglomeration in the system as a well-distributed system ensures consistent and controlled drug release, maintains formulation stability and contributes to product safety and effectiveness.[49]

3.2.4. Physical Evaluations of ZOE-Loaded NLC Gel. According to the stability investigation, the three gel formulations were stored for 90 days at 27 °C. The physical appearance of the gels exhibited only minimal changes compared to that of the NLC gel, as indicated in Table 4. After a meticulous observation period of 90 days (Figure 6),

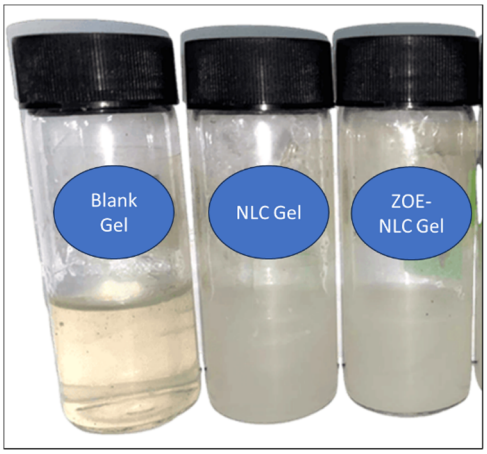

Figure 6. Physical observation of gel formulation (from the left) of blank gel, NLC gel, and ZOE-NLC gel on Day 90. Photograph courtesy of Sharifah Sarah Shazwani. Copyright 2024.

the pH of the NLC gel exhibited a modest increase of 0.5%, reaching a value of 5.74. This observation suggests that the administration of the product results in minimal skin irritation as it does not interfere with the inherent acid mantle of the skin.

The consistency of the drug content plays a significant role in both the drug dispersion inside the NLC gel system and the quantity of drug that is ultimately delivered to the skin. The investigation revealed that the NLC gel with a concentration of 76% was capable of accommodating up to 74% ZOE, while ensuring consistent dispersion of the active components throughout the system. This finding suggested that the formulation was effective in generating a uniform and consistent mixture of the two constituents, which is essential for achieving the best possible performance and effectiveness. NLC gels containing ZOE exhibited a smooth gliding property upon application to the skin and maintained a residual level of stickiness or greasiness upon drying. Owing to the thermoresponsive nature of the gels, the loaded NLC gels immediately

https://doi.org/10.1021/acsomega.4c00091
ACS Omega 2024, 9, 17379−17388

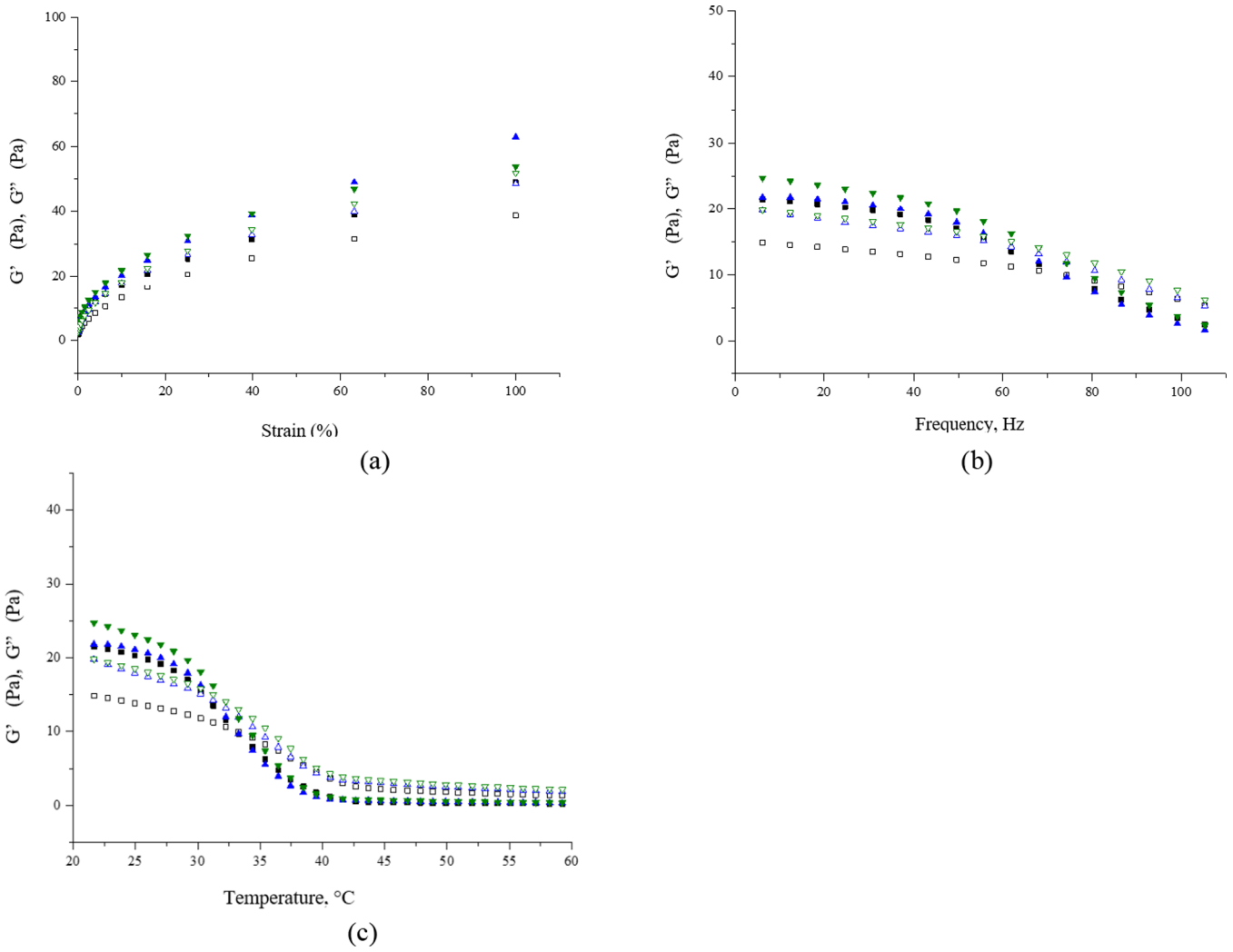

Figure 7. Rheological measurement of sample blank gel (■), NLC gel (▲), and *Z. officinale*-loaded gel (▼) with G' (solid symbol ■) and G'' (open symbol □); as a function of strain in frequency (a), amplitude (b), and temperature sweep (c).

converted from a solid-like consistency to a watery consistency upon contact with the skin.

To identify the linear viscoelastic region (LVR) and understand the mechanical properties of the gel, an amplitude sweep was conducted by systematically varying the amplitude of the applied force while measuring the response of the material. This helped to determine the strain range within which the gel exhibited linear viscoelastic behavior, indicating its ability to withstand deformation without significant structural changes.

Figure 7 presents rheological measurements of various gel samples, including a blank gel, NLC gel, and ZOE-loaded NLC gel, with a focus on frequency sweep. The frequency sweep test assesses viscoelastic behavior through the storage modulus (G') and loss modulus (G''). The ZOE-loaded NLC gel samples exhibited viscoelastic behavior similar to that of the NLC gel and blank gel, presenting solid-like properties at lower strain percentages. The addition of *i*-C enhanced the rigidity and resistance of the gel system to degradation, as observed from the crossover point at a strain of approximately 120%. The extract-loaded NLC gel demonstrated a higher G' than G'' compared to the blank and NLC gel alone, indicating the influence of the extract on the viscoelastic properties of the gel matrix.

In the amplitude sweep (Figure 7b), the behavior of the gel on different time scales and frequencies was examined. The gel samples showed poor spreadability, with G' higher than G'' across the investigated frequency range. NLCs decrease fluidity, and higher shear rates increase viscosity owing to particulate dispersion in the gel matrix. The ZOE-loaded NLC gel exhibited stronger stability than the emulsion in the gel and broke down at temperatures above 35 °C.

Temperature sweep analysis (Figure 7c) further elucidated the viscoelastic behavior, revealing that the extract-loaded NLC gel had a higher G' than G'', indicating more solid-like or elastic behavior. This enhancement is attributed to the contribution of the extract to a more interconnected and rigid network within the gel matrix, which improves its ability to store elastic energy.

As the temperature varies, phase transitions in the gel, such as melting or gelling, occur based on the composition of nanostructured lipid carriers. The acute slope in the temperature sweep graph indicates changes in the *i*-C structure, which influence the connectivity and solubility of the gel in water. The gel transitions between a firm consistency and a flowing solution during heating and cooling, highlighting its responsiveness to temperature changes.

https://doi.org/10.1021/acsomega.4c00091
ACS Omega 2024, 9, 17379−17388

4. CONCLUSIONS

This study investigated the development of an NLC system containing a ZOE enriched with flavonoids. Optimal encapsulation of ZOE within the NLC was achieved when the ZOE content was 2%. The most optimal outcomes were obtained using NLC loaded with 0.4% ZOE, with a mean particle size ranging from 302 to 344 nm and a consistently low polydispersity index (PDI) below 0.25 during the entire 28 day observation period. This study suggests the potential for producing a variety of NLC products derived from natural sources. The morphology of the ZOE-loaded NLC exhibited stability and a well-defined structure characterized by a uniform distribution of distinct particles without any evidence of aggregation. This study emphasizes the potential of the NLC gel as a carrier for ZOE, rendering it a promising option for diverse pharmaceutical and therapeutic applications.

■ ASSOCIATED CONTENT

Supporting Information

The Supporting Information is available free of charge at https://pubs.acs.org/doi/10.1021/acsomega.4c00091.

Bioconversion of rutin to quercetin, flavonoid content, HPLC chromatogram of the optimized extract of *Z. officinale*, nitric oxide (NO) scavenging percentage, encapsulation efficiency, particle size and polydispersity of NLC-loaded ZOE, and physical observation and rheological behavior of ZOE-loaded NLG gel (PDF)

■ AUTHOR INFORMATION

Corresponding Authors

Anita Marlina − *Department of Chemistry, Faculty of Science, University of Malaya, Kuala Lumpur 50603, Malaysia; Research Centre for Chemistry, National Research and Innovation Agency, South Tangerang 15314, Indonesia;* orcid.org/0000-0002-8802-3746; Email: anita.marlina@brin.go.id

Misni Misran − *Department of Chemistry, Faculty of Science, University of Malaya, Kuala Lumpur 50603, Malaysia*; Email: misni@um.edu.my

Author

Sharifah Sarah Shazwani − *Department of Chemistry, Faculty of Science, University of Malaya, Kuala Lumpur 50603, Malaysia*

Complete contact information is available at: https://pubs.acs.org/10.1021/acsomega.4c00091

Notes

The authors declare no competing financial interest.

■ ACKNOWLEDGMENTS

The authors express their gratitude to the University of Malaya for providing us with the opportunity to conduct this study. This research was financially supported by a Fundamental Research Grant Scheme (FP075-2018A).

■ REFERENCES

(1) Stoia, M.; Oancea, S. Low-molecular-weight synthetic antioxidants: classification, pharmacological profile, effectiveness and trends. *Antioxidants* **2022**, *11* (4), 638.

(2) Prabakaran, G.; Sampathkumar, P.; Kavisri, M.; Moovendhan, M. Extraction and characterization of phycocyanin from Spirulina platensis and evaluation of its anticancer, antidiabetic and antiinflammatory effect. *Int. J. Bio. Macromol.* **2020**, *153*, 256−263.

(3) Yesmin, S.; Paul, A.; Naz, T.; Rahman, A. A.; Akhter, S. F.; Wahed, M. I. I.; Emran, T. B.; Siddiqui, S. A. Membrane stabilization as a mechanism of the anti-inflammatory activity of ethanolic root extract of Choi (Piper chaba). *Clin. Phytosci.* **2020**, *6*, 59.

(4) Cai, M.; Xu, Y.-C.; Deng, B.; Chen, J.-B.; Chen, T.-F.; Zeng, K.-F.; Chen, S.; Deng, S.-H.; Tan, Z.-B.; Ding, W.-J.; Zhang, S.-w.; Liu, B.; Zhang, J.-z. Radix Glycyrrhizae extract and licochalcone a exert an anti-inflammatory action by direct suppression of toll like receptor 4. *J. Ethnopharm.* **2023**, *302*, No. 115869.

(5) Eid, O.; Elkady, W. M.; Ezzat, S.; El Sayed, A.; Abd Elsattar, E. Comprehensive Overview: The Effect of Using Different Solvents for Barley Extraction with Its Anti-Inflammatory and Antioxidant Activity. *Chem. Biodiversity* **2023**, *20* (3), No. e202200935.

(6) Cortés-Fernández, I.; Sureda, A.; Adrover, M.; Caprioli, G.; Maggi, F.; Gil-Vives, L.; Capó, X. Antioxidant and anti-inflammatory potential of rhizome aqueous extract of sea holly (Eryngium maritimum L.) on Jurkat cells. *J. Ethnopharm.* **2023**, *305*, No. 116120.

(7) Singh, S.; Chidrawar, V. R.; Hermawan, D.; Dodiya, R.; Samee, W.; Ontong, J. C.; Ushir, Y. V.; Chidrawar, V. R.; Hermawan, D.; Dodiya, R.; Samee, W.; Ontong, J. C.; Ushir, Y. V.; Prajapati, B. G.; Chittasupho, C. Hypromellose highly swellable composite fortified with Psidium guajava Leaf phenolic-rich extract for antioxidative, antibacterial, anti-inflammatory, anti-melanogenesis, and hemostasis applications. *J. Polym. Environ.* **2023**, *31*, 3197−3214, DOI: 10.1007/s10924-023-02819-9.

(8) Zhang, S.; Kou, X.; Zhao, H.; Mak, K. K.; Balijepalli, M. K.; Pichika, M. R. Zingiber officinale var. rubrum: Red Ginger's Medicinal Uses. *Molecules* **2022**, *27* (3), 775 DOI: 10.3390/molecules27030775.

(9) Wadhwa, K.; Kadian, V.; Puri, V.; Bhardwaj, B. Y.; Sharma, A.; Pahwa, R.; Rao, R.; Gupta, M.; Singh, I. New insights into quercetin nanoformulations for topical delivery. *Phytomedicine Plus* **2022**, *2* (2), No. 100257.

(10) Garg, J.; Pathania, K.; Sah, S. P.; Pawar, S. V. Nanostructured lipid carriers: a promising drug carrier for targeting brain tumours. *Future J. Pharm. Sci.* **2022**, *8* (1), 25.

(11) Cao, F.; Gui, S.-Y.; Gao, X.; Zhang, W.; Fu, Z.-Y.; Tao, L.-M.; Jiang, Z.-X.; Chen, X.; Qian, H.; Wang, X. Research progress of natural product-based nanomaterials for the treatment of inflammation-related diseases. *Mater. Design* **2022**, *218*, No. 110686.

(12) Chuang, S.-Y.; Lin, Y.-K.; Lin, C.-F.; Wang, P.-W.; Chen, E.-L.; Fang, J.-Y. Elucidating the Skin Delivery of Aglycone and Glycoside Flavonoids: How the Structures Affect Cutaneous Absorption. *Nutrients* **2017**, *9* (12), 1304 DOI: 10.3390/nu9121304.

(13) Chavda, V. P.; Patel, A. B.; Mistry, K. J.; Suthar, S. F.; Wu, Z. X.; Chen, Z. S.; Hou, K. Nano-Drug Delivery Systems Entrapping Natural Bioactive Compounds for Cancer: Recent Progress and Future Challenges. *Front. Oncol.* **2022**, *12*, No. 867655.

(14) Quach, H.; Le, T.-V.; Nguyen, T.-T.; Nguyen, P.; Nguyen, C. K.; Dang, L. H. Nano-Lipids Based on Ginger Oil and Lecithin as a Potential Drug Delivery System. *Pharmaceutics* **2022**, *14*, 1654 DOI: 10.3390/pharmaceutics14081654.

(15) Sadiah, S.; Anwar, E.; Djufri, M.; Cahyaningsih, U. Preparation and characteristics of nanostructured lipid carrier (NLC) loaded red ginger extract using high pressure homogenizer method. *J. Pharm. Sci. Res.* **2017**, *9* (10), 1889−1893.

(16) Rosli, N. A.; Islan, G. A.; Hasham, R.; Castro, G. R.; Aziz, A. A. Incorporation of Nanoparticles Based on Zingiber Officinale Essential Oil into Alginate Films for Sustained Release. *J. Phys. Sci.* **2022**, *33* (2), 107−124.

(17) Mhetre, R. M.; Waghmode, R. V.; Khyamgonde, S. S.; Nilee, R. S.; Sable, V. U.; Jadhav, R. I. Liposome: An advanced pharmaceutical carrier in novel drug delivery system. *Int. J. Sci. Res. Archive* **2023**, *10* (02), 874−894.

(18) Ng, K. S.; Mohd Zin, Z.; MohdMaidin, N.; Mamat, H.; Juhari, N. H.; Zainol, M. K. High-performance liquid chromatography (HPLC) analysis for flavonoids profiling of Napier grass herbal tea. *Food Res.* **2020**, *5*, 65−71, DOI: 10.26656/fr.2017.5(1).311.

(19) Bnyan, R.; Khan, I.; Ehtezazi, T.; Saleem, I.; Gordon, S.; O'Neill, F.; Roberts, M. Surfactant Effects on Lipid-Based Vesicles Properties. *J. Pharm. Sci.* **2018**, *107* (5), 1237−1246.
(20) Costa, R.; Costa Lima, S. A.; Gameiro, P.; Reis, S. On the Development of a Cutaneous Flavonoid Delivery System: Advances and Limitations. *Antioxidants* **2021**, *10* (9), 1376 DOI: 10.3390/antiox10091376.
(21) Gujar, K.; Wairkar, S. Nanocrystal technology for improving therapeutic efficacy of flavonoids. *Phytomedicine* **2020**, *71*, No. 153240.
(22) Madkhali, O. A. Perspectives and Prospective on Solid Lipid Nanoparticles as Drug Delivery Systems. *Molecules* **2022**, *27*, 1543 DOI: 10.3390/molecules27051543.
(23) Farhanim, M. L.; Teo, Y. Y.; Misran, M.; Suk, V. R. E.; Low, K. H. Formulation and Physicochemical Properties of Nanostructured Lipid Carriers from Beeswax and Rosemary Oil as a Drug Carrier. *Chiang Mai J. Sci.* **2020**, *47* (1), 114−126.
(24) Apostolou, M.; Assi, S.; Fatokun, A. A.; Khan, I. The Effects of Solid and Liquid Lipids on the Physicochemical Properties of Nanostructured Lipid Carriers. *J. Pharm. Sci.* **2021**, *110* (8), 2859−2872.
(25) Akombaetwa, N.; Ilangala, A. B.; Thom, L.; Memvanga, P. B.; Witika, B. A.; Buya, A. B. Current Advances in Lipid Nanosystems Intended for Topical and Transdermal Drug Delivery Applications. *Pharmaceutics* **2023**, *15*, 656 DOI: 10.3390/pharmaceutics15020656.
(26) Chaves, J. O.; de Souza, M. C.; da Silva, L. C.; Lachos-Perez, D.; Torres-Mayanga, P. C.; Machado, A. P. D. F.; Forster-Carneiro, T.; Vázquez-Espinosa, M.; González-de-Peredo, A. V.; Barbero, G. F.; Rostagno, M. A. Extraction of Flavonoids From Natural Sources Using Modern Techniques. *Front. Chem.* **2020**, *8*, No. 507887, DOI: 10.3389/fchem.2020.507887.
(27) Domínguez Moré, G. P.; Cardona, M. I.; Sepúlveda, P. M.; Echeverry, S. M.; Oliveira Simões, C. M.; Aragón, D. M. Matrix Effects of the Hydroethanolic Extract of Calyces of Physalis peruviana L. on Rutin Pharmacokinetics in Wistar Rats Using Population Modeling. *Pharmaceutics* **2021**, *13* (4), 535.
(28) Yang, J.; Lee, H.; Sung, J.; Kim, Y.; Jeong, H. S.; Lee, J. Conversion of Rutin to Quercetin by Acid Treatment in Relation to Biological Activities. *Prev. Nutr. Food Sci.* **2019**, *24* (3), 313−320.
(29) Shraim, A. M.; Ahmed, T. A.; Rahman, M. M.; Hijji, Y. M. Determination of total flavonoid content by aluminum chloride assay: A critical evaluation. *LWT* **2021**, *150*, No. 111932.
(30) Zan, L.; Song, W.; Wang, W.; He, G.; Li, X.; Pei, J. Purification, antioxidant activities, encapsulation, and release profile of total flavonoids in Peony seed meal. *Food Sci. Nutr.* **2022**, *10* (4), 1051−1057.
(31) Azieana, J.; Zainon, M. N.; Noriham, A.; Rohana, M. N. Total Phenolic and Flavonoid Content and Antioxidant Activities of Ten Malaysian Wild Mushrooms. *Open Access Library Journal* **2017**, *04*, 1−9.
(32) Ng, K. S.; Mohd Zin, Z.; MohdMaidin, N.; Mamat, H.; Juhari, N. H.; Zainol, M. K. High-performance liquid chromatography (HPLC) analysis for flavonoids profiling of Napier grass herbal tea. *Food Res.* **2020**, *5* (1), 65−71.
(33) Boora, F.; Chirisa, E.; Mukanganyama, S. Evaluation of Nitrite Radical Scavenging Properties of Selected Zimbabwean Plant Extracts and Their Phytoconstituents. *J. Food Proc.* **2014**, *2014*, No. 918018.
(34) Shazwani, S.; Misran, M. Optimization and Characterization of Fatty Acid Esters (FAES) Based Nanostructured Lipid Carrier (NLC) by Box-Behnken Analysis. *Sains Malaysiana* **2022**, *51* (7), 2119−2128.
(35) Yew, H.-C.; Misran, M.Characterization of fatty acid based nanostructured lipid carrier (NLC) and their sustained release properties. *Prog. Drug Discovery Biomed. Sci.* **2019**, *2*, 1, DOI: 10.36877/pddbs.a0000022.
(36) Ying, L.; Misran, M.Rheological and physicochemical characterization of alpha-tocopherol loaded lipid nanoparticles in thermoresponsive gel for topical application. *Malaysian J. Fund Appl. Sci.* **2017**, *13*, DOI: 10.11113/mjfas.v13n3.596.
(37) López-Bascón, M. A.; Luque de Castro, M. D. Chapter 11 - Soxhlet Extraction. In *Liquid-Phase Extraction*; Poole, C. F., Ed.; Elsevier, 2020; pp 327−354.
(38) Gao, Y.; Xia, W.; Shao, P.; Wu, W.; Chen, H.; Fang, X.; Mu, H.; Xiao, J.; Gao, H. Impact of thermal processing on dietary flavonoids. *Curr. Opinion Food Sci.* **2022**, *48*, No. 100915.
(39) Ioannou, I.; Chekir, L.; Ghoul, M. Effect of Heat Treatment and Light Exposure on the Antioxidant Activity of Flavonoids. *Processes* **2020**, *8*, 1078 DOI: 10.3390/pr8091078.
(40) Abubakar, A. R.; Haque, M. Preparation of Medicinal Plants: Basic Extraction and Fractionation Procedures for Experimental Purposes. *J. Pharm. Bioallied Sci.* **2020**, *12* (1), 1−10.
(41) Pandey, J.; Bastola, T.; Tripathi, J.; Tripathi, M.; Rokaya, R. K.; Dhakal, B.; D. C, R.; Bhandari, R.; Poudel, A. Estimation of Total Quercetin and Rutin Content in *Malus domestica* of Nepalese Origin by HPLC Method and Determination of Their Antioxidative Activity. *J. Food Quality* **2020**, *2020*, No. 8853426.
(42) Adebayo, S. A.; Ondua, M.; Shai, L. J.; Lebelo, S. L. Inhibition of nitric oxide production and free radical scavenging activities of four South African medicinal plants. *J. Inflamm. Res.* **2019**, *12*, 195−203.
(43) Klojdová, I.; Milota, T.; Smetanová, J.; Stathopoulos, C. Encapsulation: A Strategy to Deliver Therapeutics and Bioactive Compounds? *Pharmaceuticals* **2023**, *16* (3), 362 DOI: 10.3390/ph16030362.
(44) Pateiro, M.; Gómez, B.; Munekata, P. E. S.; Barba, F. J.; Putnik, P.; Kovačević, D. B.; Lorenzo, J. M. Nanoencapsulation of Promising Bioactive Compounds to Improve Their Absorption, Stability, Functionality and the Appearance of the Final Food Products. *Molecules* **2021**, *26* (6), 1547 DOI: 10.3390/molecules26061547.
(45) Shen, Y.; Zhang, N.; Tian, J.; Xin, G.; Liu, L.; Sun, X.; Li, B. Advanced approaches for improving bioavailability and controlled release of anthocyanins. *J. Controlled Release* **2022**, *341*, 285−299.
(46) Müller, R. H.; Radtke, M.; Wissing, S. A. Nanostructured lipid matrices for improved microencapsulation of drugs. *Int. J. Pharm.* **2002**, *242* (1−2), 121−128.
(47) Zhang, N.; Liu, C.; Jin, L.; Zhang, R.; Siebert, H.-C.; Wang, Z.; Prakash, S.; Yin, X.; Li, J.; Hou, D.; Sun, B.; Liu, M. Influence of Long-Chain/Medium-Chain Triglycerides and Whey Protein/Tween 80 Ratio on the Stability of Phosphatidylserine Emulsions (O/W). *ACS Omega* **2020**, *5* (14), 7792−7801.
(48) Hu, S.; Li, W. X. Influence of particle size distribution on lifetime and thermal stability of Ostwald ripening of supported particles. *ChemCatChem.* **2018**, *10* (13), 2900−2907.
(49) Ezike, T. C.; Okpala, U. S.; Onoja, U. L.; Nwike, C. P.; Ezeako, E. C.; Okpara, O. J.; Okoroafor, C. C.; Eze, S. C.; Kalu, O. L.; Odoh, E. C.; Nwadike, U. G.; Ogbodo, J. O.; Umeh, B. U.; Ossai, E. C.; Nwanguma, B. C. Advances in drug delivery systems, challenges and future directions. *Heliyon* **2023**, *9* (6), No. e17488.

https://doi.org/10.1021/acsomega.4c00091
ACS Omega 2024, 9, 17379−17388